Shrestha, Badri Bhakta; Nakagawa, Hajime; Kawaike, Kenji; Baba, Yasuyuki

Numerical Simulation on Prediction of Debris-Flow Hydrograph of Heterogeneous Bed Material and Sediment Transport in a Mountainous River

NUMERICAL SIMULATION ON PREDICTION OF DEBRIS-FLOW HYDROGRAPH OF HETEROGENEOUS BED MATERIAL AND SEDIMENT TRANSPORT IN A MOUNTAINOUS RIVER

Badri Bhakta SHRESTHA[1], Hajime NAKAGAWA[2], Kenji KAWAIKE[3] and Yasuyuki BABA[4]

[1]Student Memeber of JSCE, Graduate Student, Graduate School of Engineering, Kyoto University
(Katsura Campus, Nishikyo-ku, Kyoto 615-8540, Japan)
E-mail:badri@uh31.dpri.kyoto-u.ac.jp
[2]Member of JSCE, Professor, Disaster Prevention Research Institute, Kyoto University
(Shimomisu, Yoko-oji, Fushimi-ku, Kyoto 612-8235, Japan)
E-mail: nakagawa@uh31.dpri.kyoto-u.ac.jp
[3]Member of JSCE, Associate Professor, Disaster Prevention Research Institute, Kyoto University
(Shimomisu, Yoko-oji, Fushimi-ku, Kyoto 612-8235, Japan)
E-mail: kawaike@uh31.dpri.kyoto-u.ac.jp
[4]Member of JSCE, Assistant Professor, Disaster Prevention Research Institute, Kyoto University
(Shimomisu, Yoko-oji, Fushimi-ku, Kyoto 612-8235, Japan)
E-mail: baba@uh31.dpri.kyoto-u.ac.jp

Debris flow is composed of a dense mixture of water and sediment, and it flows down along a river at high speed. In the mountainous rivers and others, the riverbed material has a wide range of particle size distribution. Thus, the temporal variation in the particle size distribution of bed material or sediment transport is required to calculate. The numerical model to calculate the temporal variation of each particle size distribution of multiple particle size stages of riverbed material and sediment transport have been already developed, but the validity of this model is not yet checked. In this study, the validity of this model is checked through the comparison with highly precise flume experimental results. The numerical simulation and experimental works are carried out to predict debris flow hydrograph of heterogeneous bed material and sediment transport in a mountainous river. In the numerical simulation, model of a temporal variation in the particle size distribution of riverbed and flow, and the dynamic wave model for a debris flow are employed.

Key Words : *debris flow, heterogeneous sediment, simulations, experiments, riverbed grain size variation*

1. INTRODUCTION

Debris flow is composed of a dense mixture of water and sediment, and it surges down along a river at high speed, which is among the most dangerous natural hazards that affect humans and properties[1), 2), 3)]. In the mountainous rivers and others, since the riverbed material has a wide range of particle size distribution, the sediment transportation brought by flowing water sometimes becomes selective, being directed toward having the constituents of fine fractions. In such a case, there also arises the need to calculate a time like change in the particle size distribution of bed material or sediment transport[4)]. The numerical model to calculate the temporal variation of each particle size distribution of multiple particle size stages of riverbed material and sediment transport have been developed by Takahashi et al.[5)] and applied to the Camuri Grande river basin of Venezuela , but the validity of this model is not yet checked. In this study, the validity of this model is checked through the comparison with highly precise flume experimental results. It is necessary to check the validity of the model for the safe applications.

The numerical simulations and experiments are carried out to predict the debris flow hydrograph of heterogeneous bed material and sediment transport in a mountainous river. In the numerical simulation, model of a temporal variation in the particle size distribution developed by Takahashi et al.[5] and the dynamic wave model for a debris flow are employed. The range of particle size distribution is divided into multiple particle size stages. The temporal variation of each particle size distribution of riverbed material is obtained from the balance of sediment discharge in each particle size stage by means of a differential equation.

2. NUMERICAL MODEL

(1) Governing equations of the flow

The depth averaged one-dimensional momentum equation of the flow mixture is expressed as

$$\frac{\partial M}{\partial t}+\beta\frac{\partial (uM)}{\partial x}=gh\sin\theta-gh\cos\theta\frac{\partial h}{\partial x}-\frac{\tau_b}{\rho_T} \quad (1)$$

where $M\ (=uh)$ is flow flux in x direction, u is the mean velocity, h is flow depth, β is momentum correction factor equal to 1.25 for a stony debris flow[6], g is the acceleration due to gravity, θ is bed slope, ρ_T is mixture density of the debris flow ($\rho_T=\sigma C_L+(1-C_L)\rho_m$), σ is density of the sediment particle, ρ_m is density of fluid phase, τ_b is bottom shear stress described as follows[6]. For a stony debris flow ($C_L>0.4C_{*L}$)

$$\tau_b=\frac{\rho_T}{8}\left(\frac{d_{mL}}{h}\right)^2\frac{u\,|u|}{\{C_L+(1-C_L)\rho_m/\sigma\}\{(C_{*L}/C_L)^{1/3}-1\}^2} \quad (2)$$

For an immature debris flow ($0.02\le C_L\le 0.4C_{*L}$)

$$\tau_b=\frac{\rho_T}{0.49}\left(\frac{d_{mL}}{h}\right)^2u|u| \quad (3)$$

For a turbulent flow ($C_L<0.02$)

$$\tau_b=\frac{\rho g n^2 u|u|}{h^{1/3}} \quad (4)$$

where C_L is volumetric concentration of coarse particles in the flow, C_{*L} is the volumetric concentration of all the coarse particles when the bed is composed only of coarse particles, d_{mL} is average grain size of coarse fraction in the fluid, ρ is density of the water, and n is Manning's roughness coefficient.

Flow is composed of different grain size sediment particles, the extent of grain size is divided in to k_e grades and the sediment diameter of grain size class k is defined as d_k. The grain size components from grades $k=1$ to $k=k_1$ are defined as fine and considered to constitute a fluid phase. The grain size components from grades $k=k_1+1$ to $k=k_e$ are defined as coarse particles. The volumetric concentration of coarse and fine fractions, density of the fluid phase, and mean diameter of the coarse particles in the flow respectively are expressed as follows[5].

$$C_L=\sum_{k=k_1+1}^{k_e}C_k \quad (5)$$

$$C_F=\left(\sum_{k=1}^{k_1}C_k\right)/(1-C_L) \quad (6)$$

$$\rho_m=\rho+\frac{\sigma-\rho}{1-C_L}\sum_{k=1}^{k_1}C_k=\rho+(\sigma-\rho)C_F \quad (7)$$

$$d_{mL}=\left(\sum_{k=k_1+1}^{k_e}d_kC_k\right)/C_L \quad (8)$$

where C_k is volumetric concentration of grade k particles in the total water and sediment volume, and C_F is volumetric concentration of the fine particle fraction in the interstitial fluid.

The equation of continuity for total volume, the equation of continuity for each grain size class and equation for the erosion/deposition process to change in the riverbed variation respectively can be expressed as follows:

$$\frac{\partial h}{\partial t}+\frac{\partial M}{\partial x}=i_{sb}K_1 \quad (9)$$

$$\frac{\partial C_kh}{\partial t}+\frac{\partial MC_k}{\partial x}=i_{sbk} \quad (10)$$

$$\frac{\partial z_b}{\partial t}+i_{sb}=0 \quad (11)$$

where i_{sb} is erosion (>0) or deposition (≤ 0) velocity on the riverbed, i_{sbk} is erosion or deposition velocity of k[th] grade particles, z_b is erosion or deposition thickness of the bed measured from the original bed surface elevation and coefficient K_1 is described as follows:

$$K_1 = \begin{cases} C_{*L} + (1 - C_{*L})\{C_{*F} + (1 - C_{*F})s_b\}; & (i_{sb} > 0) \\ 1; \quad (i_{sb} \le 0) \end{cases} \tag{12}$$

in which C_{*F} is volumetric concentration of fine particles in static bed and s_b is degree of saturation of the bed.

(2) Model of erosion and deposition velocity

The erosion velocity equation for saturated case is used as[6)]

$$i_{sbo} = \delta_e \frac{C_{L\infty} - C_L}{C_{*L} - C_{L\infty}} \frac{M}{d_{mL}} \tag{13}$$

where i_{sbo} is erosion velocity of a riverbed of mean particle diameter d_{mL}, δ_e is erosion coefficient, and $C_{L\infty}$ is equilibrium sediment concentration. The erosion velocity for each coarse and fine grade of particle i_{sbk} can be described as follows[5)].

$$i_{sbk} = 0\,;(k > k_2) \tag{14}$$

$$i_{sbk} = i_{sbo} f_{bLk} C_{*L} \sum_{k=k_1+1}^{k_2} f_{bLk} \quad ;\ (k_1 < k \le k_2) \tag{15}$$

$$i_{sbk} = i_{sbo}(1 - C_{*L})C_{*K} \sum_{k=k_1+1}^{k_2} f_{blk} \quad ;\ (k \le k_1) \tag{16}$$

where k_2 is largest diameter of sediment particle smaller than depth of water, C_{*k} ($C_{*k} = \{C_{*L}/(1 - C_{*L})\} f_{bLk}$; $k = 1 \sim k_1$) is volumetric concentration of the fine particle in the void of the soil structure built by coarse sediment particles on the bed and f_{bLk} is the ratio of the grains in the k[th] grain size class to all coarse fractions on the surface layer of the riverbed expressed as

$$f_{bLk} = f_{bk} \Big/ \sum_{k=k_1+1}^{k_e} f_{bk} \tag{17}$$

in which f_{bk} is the ratio of the grains in the k[th] grain size class to all grains on the surface layer of the river bed.

The deposition velocity of coarse particle caused by imbalanced concentration can be expressed as

$$i_{sbo} = \delta_d \frac{C_{L\infty} - C_L}{C_{*L}} \frac{M}{h} \tag{18}$$

where δ_d is deposition coefficient.

The deposition velocity of each grade of coarse and fine sediment can be expressed as

$$i_{sbk} = i_{sbo} \frac{C_k}{C_L} C_{*L\max} \quad ;\ (k > k_1) \tag{19}$$

$$i_{sbk} = i_{sbo}(1 - C_{*L\max}) \frac{C_k}{1 - C_L} \quad ;\ (k \le k_1) \tag{20}$$

where $C_{*L\max}$ is volumetric concentration of the coarse particles in the maximum compacted state.

Erosion and deposition velocities in bulk that include void space i_{sb} are given as

$$i_{sb} = \frac{1}{C_{*L}} \sum_{k=k_1+1}^{k_e} i_{sbk} \qquad \text{(for erosion)} \tag{21}$$

$$i_{sb} = \frac{1}{C_{*L\max}} \sum_{k=k_1+1}^{k_e} i_{sbk} \quad \text{(for deposition)} \tag{22}$$

The equilibrium sediment concentration of coarse fraction $C_{L\infty}$ can be described as follows[7)]. If $\tan\theta_w > 0.138$

$$C_{L\infty} = \frac{\rho_m \tan\theta_w}{(\sigma - \rho_m)(\tan\phi - \tan\theta_w)} \tag{23}$$

If $0.03 < \tan\theta_w \le 0.138$

$$C_{L\infty} = 6.7 \left\{ \frac{\rho_m \tan\theta_w}{(\sigma - \rho_m)(\tan\phi - \tan\theta_w)} \right\}^2 \tag{24}$$

If $\tan\theta_w \le 0.03$

$$C_{L\infty} = \frac{(1 + 5\tan\theta_w)\tan\theta_w}{\sigma/\rho_m - 1} \left(1 - \alpha_0^2 \frac{\tau_{*c}}{\tau_*}\right)\left(1 - \alpha_0^2 \sqrt{\frac{\tau_{*c}}{\tau_*}}\right) \tag{25}$$

$$\alpha_0^2 = \frac{2\{0.425 - (\sigma/\rho_m)\tan\theta_w /(\sigma/\rho_m - 1)\}}{1 - (\sigma/\rho_m)\tan\theta_w /(\sigma/\rho_m - 1)} \quad (26)$$

$$\tau_{*_c} = 0.04 \times 10^{1.72\tan\theta_w} \quad (27)$$

$$\tau_* = \frac{h\tan\theta_w}{(\sigma/\rho_m - 1)d'_{mL}} \quad (28)$$

where τ_{*_c} is the non-dimensional critical shear stress, τ_* is the non-dimensional shear stress, d'_{mL} is the mean diameter of movable coarse particles on the riverbed, θ_w is water surface gradient, and ϕ is internal friction angle of sediment particles.

(3) Model of variation of riverbed grain size

The temporal variation in the volume fraction of k^th^ grade sediment particles in the surface layer expressed by f_{bk} for the erosion and deposition can be expressed as follows. For erosion:

$$\frac{\partial f_{bk}}{\partial t} = \frac{i_{sb} J_0 f_{0k} - i_{sbk} - i_{sb}(J_0 - J) f_{bk}}{\delta_m J} \quad (29)$$

For deposition:

$$\frac{\partial f_{bk}}{\partial t} = \frac{-i_{sbk} + i_{sb} C_* f_{bk}}{\delta_m J} \quad (30)$$

where $J = C_{*L} + (1 - C_{*L})C_{*F}$ is sediment concentration in the surface layer, $J_0 = C_{*L0} + (1 - C_{*L0})C_{*F0}$ is the sediment concentration in the lower layer, δ_m is the thickness of the surface layer, f_{0k} is the volume fraction of k^th^ grade sediment particles in the lower layer.

3. LABORATORY EXPERIMENTS

A rectangular flume of 5m long, 10cm wide and 13cm deep is used for the experiments. The slope of flume is set at 18 degrees. The details of experiment flume setup are shown in **Fig.1**. The bed sediment with 1.9m long and 7cm deep is positioned 2.8m upstream from the outlet of the flume by installing a partition of 7cm in height to retain the sediment. This sediment bed is saturated by water. The bed sediment material is composed of eight grain-size classes. The experimental works are carried out for three types of bed sediments (bed sediment-A, bed sediment-B and bed sediment-C). Silica sand of nearly uniform distributed six grain size classes (S1, S2, S3, S4, S5, S6) of mean diameter (4.26mm, 2.56mm, 1.85mm, 0.94mm, 0.67mm, 0.29mm) in proportion (1.5, 1.5, 1, 1, 1, 0.7) and gravel of nearly uniform distributed two grain size classes (G1, G2) of mean diameter (9.0mm, 14.70mm) in proportion (1.5, 1) by weight are mixed to prepared bed sediment-A. Silica sand (S1, S2, S3, S4, S5, S6) and gravel (G1, G2) are mixed in equal proportion by weight to prepared bed sediment-B. Silica sand (S1, S2, S3, S4, S5, S6) in proportion (1, 1, 1, 2, 2, 2) and gravel (G1, G2) in proportion (1, 1) by weight are mixed to prepared bed sediment-C. **Fig.2** shows the particle size distribution of each of eight grain size classes of silica sand and gravel. **Fig.3** shows particle size distribution of the prepared bed material, bed sediment-A, bed sediment-B and bed sediment-C. Sediment materials with maximum sediment concentration $C_* = 0.65$, angle of repose $\tan\phi = 0.7$

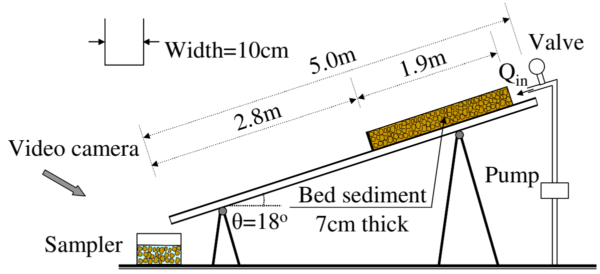

Fig.1 Experimental flume setup.

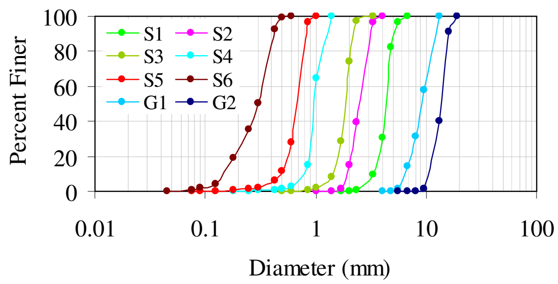

Fig.2 Partical size distribution of each of eight grain size classes.

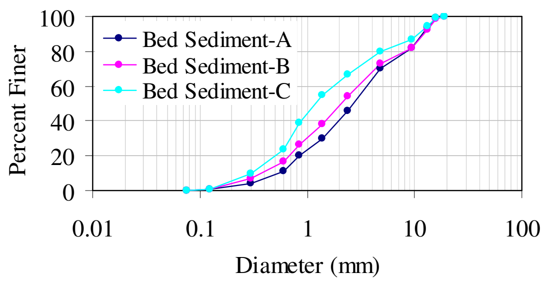

Fig.3 Particle size distribution of prepared bed sediments.

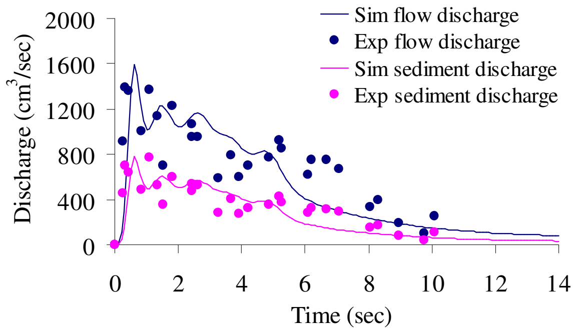

Fig.4 Flow and sediment discharge at downstream end of the flume, Bed Sediment-A.

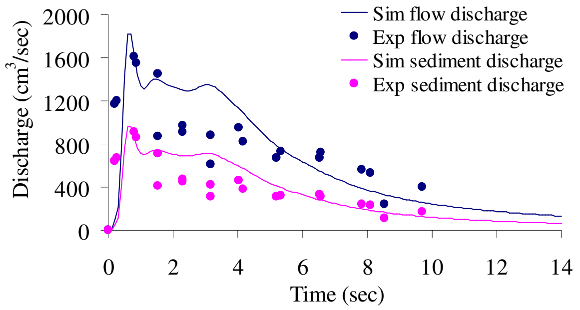

Fig.6 Flow and sediment discharge at downstream end of the flume, Bed Sediment-B.

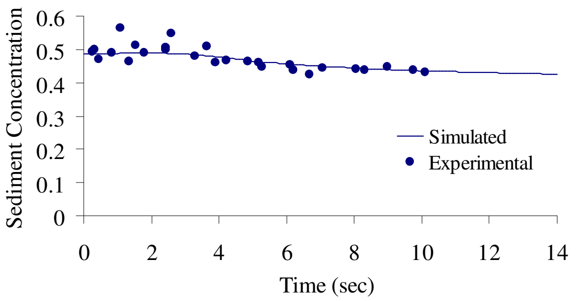

Fig.5 Sediment concentration of debris flow at downstream end of the flume, Bed Sediment-A.

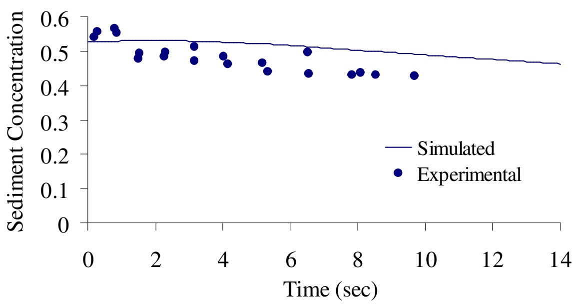

Fig.7 Sediment concentration of debris flow at downstream end of the flume, Bed Sediment-B.

and sediment density $\sigma =$ 2.65g/cm^3 are used. Debris flow is produced by supplying a constant water discharge at a rate of 260cm^3/sec for 10sec from the upstream end of the flume. Debris flow produced in the experiments is the fully stony type debris flow and the largest particles are accumulated in the forefront. Debris flow discharge is collected using manually movable sampler boxes. Total flow discharge and sediment discharge are calculated on the basis of the residence time of each box under the flume mouth which is determined by analyzing the images shot by a video camera located above the flume end. Grain size analyses are carried out to measure the mean diameter and particle size distribution of collected sediment outflow in the each sampler boxes.

4. RESULTS AND DISCUSSIONS

Numerical simulations and experiments are carried out to predict debris flow hydrograph of mixed sediment material with temporal variations of particle size distribution of bed material and sediment flow. The calculation conditions of the numerical simulations are as follows; the grid size Δx =10cm, the time interval $\Delta t =$ 0.001sec, $\rho =$ 1.0g/cm^3, $C_{*L} = C_{*F} = C_{*L\max} = C_{*F\max} =$ 0.65, $\delta_m =$ 7.0cm, the degree of saturation s_b =1.0, Manning's roughness $n = 0.04$, erosion coefficient δ_e =0.008 and deposition coefficient δ_d =0.01. The drop flow equation of $M = h\sqrt{2gh}$ is used for the outflow condition at the downstream end of the flume. The number of particle grain-size grades is divided in eight numbers ($k_e = 8$) and grade of fine particle that is assumed to behave like fluid is grade 1 ($k_1 = 1$) of particle size 0.29mm. A transition in the reach from the erodible sediment bed to the rigid bed is considered to be gradual even there is actually an abrupt drop of 7cm.

Fig.4 shows the simulated and experimental results of temporal variations of flow and sediment discharge at downstream end of the flume in the case of bed sediment-A. The results of discharge hydrographs in **Fig.4** show that the peak discharge of the debris flow is far larger than the supplied water discharge at the upstream end because the erosion of riverbed sediment by the flow increases the discharge of the flow. The temporal change in the sediment concentration of the debris flow discharge is shown in **Fig.5**, and the sediment concentration is found higher in frontal part of the flow.

The simulated and experimental results of temporal variation in the outflow discharge and sediment concentration at downstream end of the

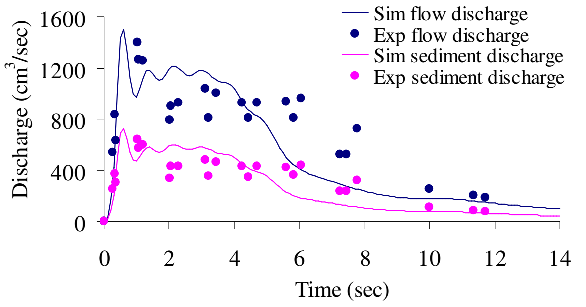

Fig.8 Flow and sediment discharge at downstream end of the flume, Bed Sediment-C.

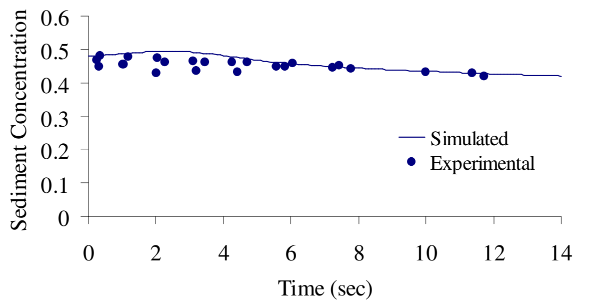

Fig.9 Sediment concentration of debris flow at downstream end of the flume, Bed Sediment-C.

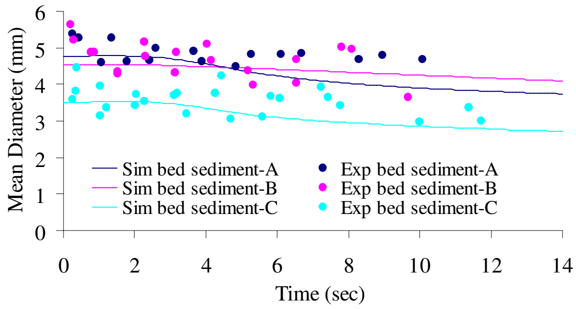

Fig.10 Mean diameter of run out sediment at downstream end of the flume.

flume in the case of bed sediment-B respectively are shown in **Fig.6** and **Fig.7**. In the case of bed sediment-C, the simulated results are found more approximate with experimental results with erosion coefficient δ_e =0.004, because of the smaller particles contains higher in this bed sediment than the other two types of bed sediment, which may be required smaller erosion coefficient, and the results of outflow discharge and sediment concentration respectively are shown in **Fig.8** and **Fig.9**. The simulated and experimental results of the temporal changes of mean diameter of the run out sediments at downstream end of the flume are shown in **Fig.10**, which shows large particles gather at the front part of the flow. The sediment concentration as well as the content of the larger particles at the front increases as the debris flow continues to move downstream. The simulated results agree well with the experimental results.

5. CONCLUSIONS

The numerical simulations are performed for flume experimental cases to predict debris flow hydrograph of heterogeneous bed material or sediment transport. The numerical results are in good agreement with the experimental results. The numerical model described in this paper could reproduce the experimental results of debris flow hydrograph and the temporal variation of mean diameter of run out sediment at downstream end, and it is useful for the prediction of debris flow in a mountainous river and others, where riverbed has wide range of particle size distribution. The prediction of debris flow hydrograph can be useful for manage the sediment disaster in the downstream area. The temporal variation in grain size distribution of the bed material and flow can be calculated by the model of grain size distribution used. The simulated and experimental results of flow and sediment discharge, sediment concentration, and variation in mean diameter at downstream end of the flume are quite close to each other.

ACKNOWLEDGMENT: Dr. Hao Zhang, Assistant Professor, Disaster Prevention Research Institute, Kyoto University, Japan, is gratefully acknowledged for his suggestions in many ways.

REFERENCES

1) Takahashi, T.: Initiation and flow of various types of debris-flow, Proc., 2nd Conf. on Debris-Flow Hazards Mit.: Mech., Pred., and Assessment, pp. 15-25, 2000.
2) Takahashi, T.: Debris Flow: Mechanics, Prediction and Countermeasures, Taylor & Framcis/Balkeman, 2007.
3) Armanini, A. and Gregoretti, C.: Triggering of debris-flow by overland flow: A comparison between theoretical and experimental results, Proc., 2nd Conf. on Debris-Flow Hazards Mit.: Mech., Pred., and Assessment, pp. 117-124, 2000.
4) Nakagawa, H., Satofuka, Y. and Takahama, J.: Water Induced Hazard–I, Sub Text Book, M. Sc. in Water Resources Engineering, Institute of Eng., Nepal, 2002.
5) Takahashi, T., Nakagawa, H., Satofuka, Y., and Kawaike, K.: Flood and sediment disasters triggered by 1999 rainfall in Venezuela; A river restoration plan for an alluvial fan, *J. of Natural Disaster Science*, Vol. 23, No. 2, pp. 65-82, 2001.
6) Takahashi, T., Nakagawa, H., Harada, T., and Yamashiki, Y.: Routing debris flows with particle segregation, *J. of Hyd. Eng.*, ASCE, Vol. 118, No. 11, pp. 1490-1507, 1992.
7) Nakagawa, H., Takahashi, T., Satofuka, Y., and Kawaike, K.: Numerical simulation of sediment disasters caused by heavy rainfall in Camuri Grande basin, Venezuela 1999, Proc., 3rd Conf. on Debris-Flow Hazards Mit.: Mech., Pred., and Assessment, pp. 671-682, 2003.